Automatic livestock dimension measurement driven by omnidirectional scanning selective state-space segmentation

Kai Zhang[1,2], Qin Ma[1,2*], Xiaochen Shi[1,2]

(1. *College of Information and Electrical Engineering, China Agricultural University, Beijing 100083, China*;
2. *Integrated Scientific Experimental Base for Precision Agriculture Technology of the Ministry of Agriculture and Rural Affairs (Animal Husbandry), Beijing 100097, China*)

Abstract: Existing methods often struggle to accurately and automatically separate livestock from complex background environments and are further hindered by severe noise interference in point cloud data, which leads to insufficient segmentation accuracy and ultimately affects the precision of livestock body measurements. To address these challenges, this study proposes a livestock body measurement method based on omnidirectional spatial localization segmentation. First, an omnidirectional point cloud segmentation model (Omni-PointMamba) was designed, which adopts an eight-directional scanning strategy in 3D space and an alternating dual-module architecture that integrates Point Mamba Blocks with convolutional modules. By enhancing spatial neighborhood modeling capabilities, the model efficiently fuses region-specific geometric features with comprehensive structural context, thereby achieving precise separation of livestock from background interference. Second, a spatial localization-based measurement method was developed. This method constructs a spatial coordinate system using ground normal vectors to achieve automatic rotation and alignment of the point cloud. It employs a two-step clustering strategy to identify key body parts, including the head and tail, and determines measurement landmarks through geometric point distribution analysis, enabling accurate, non-contact estimation of body size parameters. Experiments conducted on 20 pigs and 103 cattle demonstrate that the proposed model achieves outstanding segmentation performance, with mean Intersection over Union (mIoU) values of 0.9930 for pigs and 0.9685 for cattle. Furthermore, the model yields low mean absolute percentage errors (MAPE) in morphological measurements. For pigs, the MAPE for body width, hip width, and chest girth are 1.34%, 1.99%, and 1.37%, respectively. For cattle, the MAPE for body slant length, chest width, hip height, and heart girth are 2.24%, 3.28%, 2.18%, and 4.22%, respectively. These results indicate that the proposed method provides highly accurate segmentation and morphological measurement capabilities for both pigs and cattle.

Keywords: point cloud segmentation, deep learning, selective state space, livestock body measurement
DOI: 10.25165/j.ijabe.20261903.9846

Citation: Zhang K, Ma Q, Shi X C. Automatic livestock dimension measurement driven by omnidirectional scanning selective state-space segmentation. Int J Agric & Biol Eng, 2026; 19(3): 99–109.

1 Introduction

Livestock body measurement serves as a standardized monitoring approach for collecting essential growth and reproduction data in smart farming. It provides critical technical support for building automated monitoring systems for species such as pigs and cattle. Body measurements not only offer direct insight into an animal's daily health status but also play an important role in applications such as intelligent feeding strategy optimization, dynamic group management, and early warning of disease risks[1-3]. The resulting data form a reliable foundation for key aspects of smart farming, including growth modeling and genetic selection, thereby promoting the transformation of the livestock industry toward greater automation, precision, and intelligence[4,5].

In 2D image-based measurement, body traits are typically inferred from geometrically calibrated pixels and landmark localization[6-9]. However, pixel-to-metric conversion is highly sensitive to calibration errors and viewpoint changes, while keypoint inaccuracies accumulate under occlusion and pose variation, leading to unstable estimation. These limitations have motivated 3D point-cloud-based approaches, which enable direct geometric computation in physical coordinates and provide more robust spatial representations for body trait extraction[10].

In this context, effectively encoding features with complex geometric structures and accurately segmenting livestock are key steps in improving three-dimensional (3D) livestock body measurements. As a prerequisite to 3D body measurements, the quality of point cloud segmentation directly determines the precision with which traits such as body height, body length, and chest width are extracted. Only when the livestock target is fully and accurately separated from a complex background can geometric calculations be reliably performed in 3D space. In contrast to manual annotation or heuristic algorithms, deep learning methods can learn anatomical priors from large-scale datasets, reducing subjectivity and limitations associated with handcrafted rules.

Tailored solutions have been developed for various species, including dairy cattle, pigs, and sheep, demonstrating notable improvements in segmentation accuracy and robustness to posture variability. Yang et al. developed a portable smartphone system for measuring dairy cattle, reconstructing 3D point clouds from multi-angle images and applying segmentation techniques to isolate the cattle body while recovering occluded regions[11]. Morphological

Received date: 2025-06-20 **Accepted date:** 2026-04-01
Biographies: Kai Zhang, PhD candidate, research interest: Point cloud segmentation, Email: b20223080672@cau.edu.cn; **Xiaochen Shi**, PhD candidate, research interest: computer vision, small sample learning, Email: sxc@cau.edu.cn.
***Corresponding author: Qin Ma**, Associate Professor, research interest: computer vision, College of Information and Electrical Engineering, China Agricultural University, Beijing 100083, China. Tel: +86-13391809180, Email: maq782003@cau.edu.cn.

traits such as body height and body length were then automatically calculated based on the completed point cloud. Wang et al. introduced the Pig Back Transformer model for pig body measurements, which localized key anatomical landmarks in 3D point clouds using a combination of edge features and global structure[12]. Du et al. presented a 2D–3D fusion-based body measurement method, where key measurement points were detected on RGB images using a deep learning model[13]. Li et al. addressed pose sensitivity and localization issues in cattle point cloud measurement by segmenting the head, torso, and legs, then extracting pose-related features[14]. A posture correction model was applied to calibrate body diagonal length, height, and chest girth, effectively mitigating the impact of variable standing positions on measurement accuracy.

The advancement of deep learning has introduced a wide range of solutions for point cloud segmentation, providing robust technical support for non-contact livestock body measurements. These methods can be broadly categorized into five mainstream architectural paradigms: multilayer perceptron (MLP)-based[15], point convolution-based[16,17], graph learning-based[18,19], transformer-based[20,21], and state-space model-based[22] methods. Specifically, MLP-based methods (e.g., PointNet and PointNet++) process irregular point cloud data using MLPs to extract features. In contrast, point convolution-based methods adapt convolution kernels to the irregularity of point clouds, enabling local feature extraction and semantic segmentation. Graph learning-based models enhance 3D spatial geometry representation by constructing graph structures to aggregate local features. Transformer-based models leverage self-attention mechanisms to capture global and local point associations for segmentation. Notably, state-space model-based methods convert disordered point clouds into sequence structures, utilizing sequence modeling capabilities of state-space models to efficiently model global point cloud features. Liang et al. proposed PointMamba, which maps point clouds into sequences and employs a linear-complexity Mamba encoder as the backbone for global context modeling, significantly reducing computational and memory requirements[23]. Zhang et al. further introduced Point Cloud Mamba, which arranged points into spatially ordered sequences, explored multiple spatial traversals, and integrated feature guidance with spatial encoding to capture global structures efficiently[24].

Despite their wide application, existing deep learning methods for livestock point cloud segmentation still face significant limitations when applied across diverse species and environments. The anatomical complexity of livestock bodies makes it difficult to effectively integrate local geometric features with global contextual information. MLP-based and point convolution-based methods tend to be sensitive to non-rigid deformations, while graph-based models are constrained by their local topological modeling capacity. Transformer-based architectures, while powerful, often lack anatomical priors, resulting in imprecise boundary segmentation around critical measurement regions.

To address these challenges, this study proposes a two-stage measurement framework that integrates global–local feature modeling with spatial localization. At its core is an omnidirectional point cloud segmentation model (Omni-PointMamba), which innovatively combines a directionally driven Point Mamba Block with a Convolution Block (Conv Block). This design alleviates sensitivity to non-rigid deformations and compensates for the absence of anatomical priors. The Point Mamba Block, grounded in a state-space sequence model, captures global anatomical structures even amid noise, while the Conv Block aggregates multi-scale local neighborhoods to suppress fine-grained sensor noise. Building on segmentation results, a spatial localization-based measurement method is developed: it employs a two-step clustering strategy to automatically identify and precisely measure key anatomical regions (e.g., head and torso) after point cloud alignment.

The main contributions of this paper are as follows:

1) A novel livestock body measurement framework that combines an omnidirectional point cloud segmentation model (Omni-PointMamba) with a spatial localization-based measurement strategy. The framework significantly enhances segmentation accuracy and enables automated measurements of livestock point cloud data.

2) The proposed Omni-PointMamba employs an eight-directional scanning strategy in 3D space to effectively integrate global-local features. In addition, the spatial localization measurement method leverages ground normal vectors to normalize livestock point clouds and estimate livestock body measurement parameters automatically.

3) Experiments on 20 pigs and 103 cattle demonstrate that the proposed framework achieves high accuracy and strong cross-species generalizability, validating its reliability for non-contact, precise livestock body measurements in real-world farming settings.

2 Materials and methods

2.1 Data acquisition and processing for 3D point clouds

In this study, the proposed model was evaluated using 3D point-cloud datasets of two domestic animal species, namely Landrace pigs and Hereford cattle. As illustrated in Figure 1, the Landrace pig dataset was acquired using an ASUS Xtion PRO LIVE depth camera mounted on a movable metal bracket. The sensor was positioned approximately 1.5 m above the ground, providing coverage of an effective acquisition area of approximately 4 m^2. Data collection was conducted in a closed pigsty environment to minimize interference from ambient illumination on infrared depth imaging[25]. The Hereford cattle dataset was synchronously captured using three Microsoft Kinect v2 RGB-D cameras within a confined channel environment. Two side-view cameras were installed on the left and right sides of the channel at a distance of approximately 2.0 m from the animals, while a top-view camera was mounted above the channel at a height of approximately 3.0 m to enhance coverage of the dorsal and upper body regions[26].

a. Collection scene of pigs[25] b. Collection scene of cattle[26]

Figure 1 Point cloud datasets of livestock

After obtaining the experimental datasets, manual annotation was performed on the pig and cattle point clouds using CloudCompare. Specifically, point cloud cropping and merging were first conducted in CloudCompare to remove irrelevant regions and integrate multi-view point cloud information prior to annotation. Based on the processed point clouds, point-level labels were assigned by jointly considering RGB color information and geometric boundary cues in 3D space, and all points were categorized into two classes: livestock and ground background. In particular, the boundary between the livestock body and the ground background was determined mainly according to relative elevation differences, changes in local geometric continuity between the raised body contour and the relatively planar ground surface, and the distribution patterns of neighboring points in transition regions. For regions with ambiguous boundaries or sparse local point distributions, the final labels were determined by jointly considering the spatial arrangement of neighboring points and the overall body structure of the livestock, so as to ensure the rationality and consistency of the annotations as much as possible.

2.2 Overview of Omni-PointMamba

Following the above preprocessing, the Landrace pig and the Hereford cattle 3D point cloud datasets were constructed. In order to effectively segment the livestock and ground background information, the Omni-PointMamba was proposed, which is based on Omni-directional Scanning Selective State Space; its detailed architecture is illustrated in Figure 2. The core components of Omni-PointMamba encompass the Token embedding layer, Conv block, Point Mamba block, and Point prediction layer.

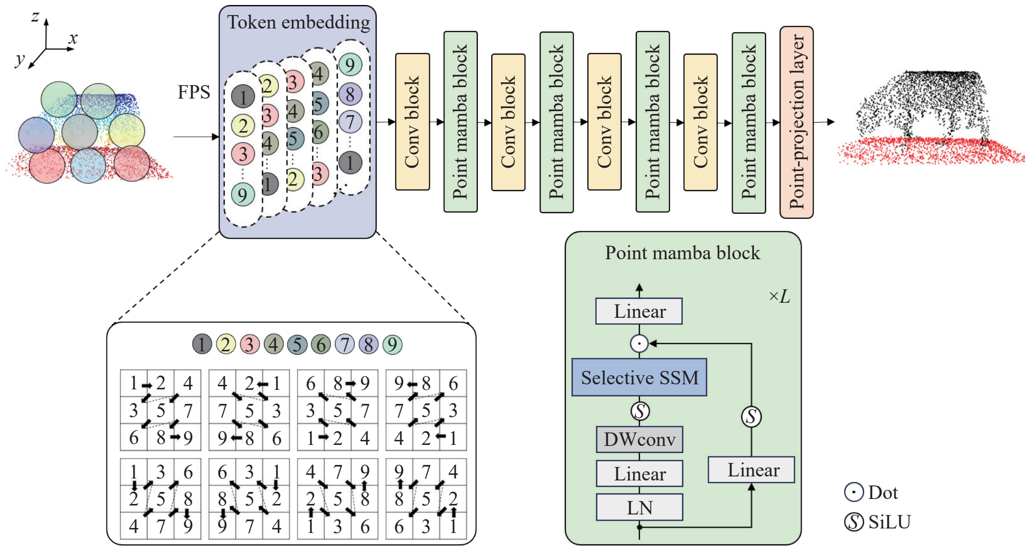

Figure 2 The structure of Omni-PointMamba

Specifically, let $p \in \mathbb{R}^{M\times3}$ denote the input point cloud, where M represents the number of points. Firstly, the Farthest Point Sampling (FPS) algorithm is adopted to select N key points from the point cloud input as the initial point features $p' \in \mathbb{R}^{N\times3}$. Subsequently, the Token embedding layer is employed to capture the sequence features in different directions, yielding the corresponding N patches. After that, the sequence features are passed through the Conv block and the Point Mamba block to capture the local and global features in the point cloud data, respectively. By concatenating these features, the fused local and global features $G_l \in \mathbb{R}^{8N\times H}$ are obtained. Finally, the Point prediction layer is utilized to output the segmentation prediction result $Y \in \mathbb{R}^{M\times C}$ for each point, where C is the number of segmentation categories.

2.2.1 Token embedding layer

To effectively extract spatial information from unordered point clouds, an omnidirectional scanning strategy is proposed, which overcomes the problem of insufficient flexibility caused by the fixed path of the traditional Hilbert scanning. This strategy adapts more effectively to the spatial distribution of point cloud data and enhances the model's capacity to capture local adjacency relationships. It performs sequential scanning along eight diagonal directions on the sampled key point data $p' \in \mathbb{R}^{N\times3}$ in 3D space, capturing the sequence features in different directions within the point cloud data.

Specifically, a set of direction vectors $D=\{d_j|j=1,2,\dots,8\}$ with eight diagonal directions is defined, where each direction $d_j=[x,y,z]$ represents a diagonal direction in 3D space with each component taking values of either +1 or −1. Then, the k-nearest neighbors (kNN) algorithm is adopted to search for the neighborhood feature set for each point in $p' \in \mathbb{R}^{N\times3}$, resulting in N patches. These neighborhood feature sets are denoted as $\mathcal{N}_{d_j}=\{N_{d_j}\in\mathbb{R}^{K\times3}|j=1,2,\dots,8\}\in\mathbb{R}^{N\times K\times3}$, where K represents the neighboring points. Subsequently, the neighborhood feature set $\mathcal{N}_{d_j}$ of the N patches is rearranged for the neighborhood feature points along each direction $d_j \in D$, and a lightweight multilayer perceptron (MLP) is employed to map the rearranged feature vectors to directional sequence feature outputs of N patches $\{P_{d_j}\in\mathbb{R}^{N\times H}|j=1,2,\dots,8\}$, where H is the output feature dimension. The formula is as follows:

$$P_{d_j}=\gamma\left(\max_{d_j\in D}\{\mathrm{Linear}(\mathcal{N}_{d_j})\}\right) \tag{1}$$

where $\gamma(\cdot)$ is a continuous function, and $\max(\cdot)$ is maximum pooling, which takes multiple vectors as input and returns a vector with element-wise maximum values.

2.2.2 Conv block for local feature

To better aggregate local features, the Conv block that uses point-wise convolution to perform mapping with the sequence features P_{d_j} of N patches as the input is proposed. Its mathematical description is as follows:

$$F_{d_j}^{Up}=\mathrm{SiLU}\left(\phi^{Up}(P_{d_j})\right) \tag{2}$$

where $\phi^{Up}(\cdot)$ represents the point-wise convolution operation, and $\mathrm{SiLU}(\cdot)$ is the SiLU activation function. Through Equation (2), the sequence feature input P_{d_j} is mapped to a higher dimension as $F_{d_j}^{Up}\in\mathbb{R}^{N\times Q}$ $(Q>H)$. Then, a similar operation is adopted to reduce the dimension of $F_{d_j}^{Up}$ back to the original dimension, and the local feature output of N patches is obtained as $F_{d_j}^{Down}\in\mathbb{R}^{N\times H}$. Therefore, the overall local feature output of N patches in eight different directions can be denoted as G, and $\mathcal{F}=concat\left(F_{d_1}^{Down},F_{d_2}^{Down},\dots,F_{d_8}^{Down}\right)\in\mathbb{R}^{8N\times H}$.

2.2.3 Point Mamba block for global feature

To extract global features and further integrate local and global representations, L Point Mamba blocks are employed to capture global spatial structural information. Each Point Mamba block is composed of layer normalization (LN), selective state space model (Selective SSM), depth-wise convolution (DWconv), and residual connections. The Point Mamba block integrates local and global features through Selective SSM, enabling the model to capture long-range dependencies and complex spatial structures within the point cloud. The corresponding mathematical formulation is as follows:

$$G_{d_j} = \gamma \odot \frac{F_{d_j}^{Down} - \mu}{\sqrt{\sigma^2 + \varepsilon}} + \beta \tag{3}$$

where, $\odot$ denotes the Hadamard Product, and $\varepsilon \to 0^+$ is an extremely small parameter approaching zero, which is used for numerical stability. $\gamma \in \mathbb{R}^H$ and $\beta \in \mathbb{R}^H$ are learnable scaling and offset parameters. $\mu \in \mathbb{R}^H$ and $\sigma^2 \in \mathbb{R}^H$ are the mean and variance of the input $F_{d_j}^{Down}$, respectively. $G_{d_j} \in \mathbb{R}^{N\times H}$ represents the features that ensure the integrity of spatial information in the d_j direction in the same centered manner. Therefore, the feature outputs across all eight directions are concatenated as $\mathcal{G} = concat\left(G_{d_1}, G_{d_2}, \ldots, G_{d_8}\right) \in \mathbb{R}^{8N\times H}$.

Subsequently, depth-wise convolution and skip connections are utilized to extract features, and their mathematical representation is as follows:

$$\mathcal{G}'_{l-1} = \mathrm{LN}(\mathcal{G}_{l-1}) \tag{4}$$

$$\mathcal{G}'_l = \mathrm{SiLU}\left(\mathrm{DWConv}\left(\mathrm{Linear}\left(\mathcal{G}'_{l-1}\right)\right)\right) \tag{5}$$

where, $\mathrm{LN}(\cdot)$ represents the layer normalization, $\mathrm{DWConv}(\cdot)$ denotes the depth-wise convolution, and $\mathcal{G}_l \in \mathbb{R}^{8N\times H}$ is the output of the (l)-th Point Mamba block.

In addition, the Selective SSM is further employed to enhance sequence modeling by introducing a continuous state space that captures long-range dependencies among sequence elements. The specific formula is shown as follows:

$$\mathcal{G}''_l = \mathrm{SiLU}\left(\mathrm{Linear}\left(\mathcal{G}'_{l-1}\right)\right) \tag{6}$$

$$\mathcal{G}_l = \mathrm{Linear}\left(\mathrm{SelectiveSSM}\left(\mathcal{G}'_l\right) \odot \mathcal{G}''_l\right) + G_{l-1} \tag{7}$$

Building upon the idea of the SSM[27], the model can map the input state $x(t)$ to the output state $y(t)$ through an intermediate hidden state $h(t) \in \mathbb{R}^H$. This state space formulation enables the modeling of sequential dependencies over time and is defined as follows:

$$h(t) = Ah(t-1) + Bx(t) \tag{8}$$

$$y(t) = Ch(t) + D \tag{9}$$

where, $h(t-1)$ represents the previous hidden state, and $x(t) \in \mathbb{R}^{Q\times H}$ denotes the input feature at time step t, and the output $y(t) \in \mathbb{R}^H$ corresponds to the output feature at the same time step. In the above formulation, $A \in \mathbb{R}^{H\times H}$ represents the state transition matrix that governs the temporal evolution of hidden states, while $B \in \mathbb{R}^H$ and $C \in \mathbb{R}^H$ denote learnable project parameters for the input and hidden states, and $D \in \mathbb{R}^H$ acts as the residual connection to preserve original input information.

2.2.4 Point-projection layer

In the last layer of the Omni-PointMamba model, the Point-projection layer is employed to generate segmentation prediction results for each sampled point. Specifically, the Point-projection layer consists of two Linear layers and one BatchNorm layer; it can be shown as follows:

$$y = \mathrm{BatchNorm}\left(\mathrm{Linear}(\mathcal{G}_l)\right) \tag{10}$$

$$Y = \mathrm{Linear}(y) \tag{11}$$

where $Y \in \mathbb{R}^{M\times C}$ corresponds to the final prediction result of the input point cloud data p, M is the total number of samples, and C is the number of categories.

2.3 Livestock body measurement

Within the normalized anatomical coordinate system, body measurement keypoints are defined based on the geometric boundary characteristics of the livestock point cloud. The coordinate system is constructed such that the longitudinal body axis aligns with the x-axis, the lateral direction with the y-axis, and the vertical direction with the z-axis. For lateral width estimation, keypoints are determined as extremal boundary points along the y-axis within anatomically localized regions. In the shoulder (i.e., anterior trunk) region, the points with the minimum and maximum y-coordinates are denoted as α_0 and α_1, representing the leftmost and rightmost anatomical boundaries, respectively. Similarly, in the hip region, the lateral extremal points along the y-axis are denoted as b_0 and b_1. As illustrated in Figure 3 and Figure 4, each point pair defines the transverse anatomical span used to compute shoulder width and hip width.

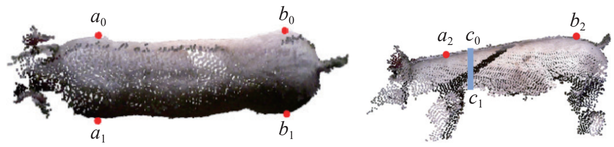

a. Measurement key points of pigs from a top view

b. Measurement key points of pigs from a side view

Note: In Figure 3a, α_0 and α_1 are the key points used for body width estimation, whereas b_0 and b_1 are the key points used for hip width estimation. In Figure 3b, c_0 and c_1 are used to determine the chest-circumference measurement, whereas α_2 and b_2 are marked as auxiliary reference points.

Figure 3 Diagram of key points of pig body measurement

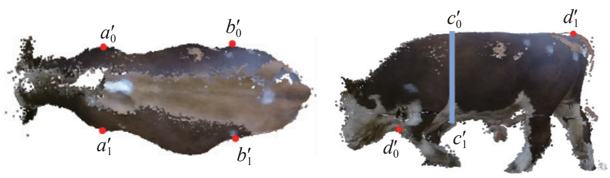

a. Measurement key points of cattle from a top view

b. Measurement key points of cattle from a side view

Note: In Figure 4a, α'_0 and α'_1 denote the key points used for chest width estimation, whereas d'_0 and d'_1 denote the key points used for body oblique length estimation. In Figure 4b, d'_1 denotes the key point used for hip height measurement, whereas the cross-section defined by c'_0 and c'_1 is used for heart girth estimation.

Figure 4 Diagram of key points of cattle body measurement

For chest circumference estimation, a reference line segment is defined within the trunk region immediately posterior to the forelimbs. Specifically, in this localized anatomical zone, a line segment parallel to the vertical axis (z-axis) is constructed to characterize the dorsoventral extent of the thoracic region. This segment serves as the central geometric reference for constructing a transverse cross-sectional plane perpendicular to the longitudinal body axis. The intersection between this plane and the livestock point cloud forms a closed contour, and the chest circumference is calculated as the perimeter of the resulting cross-sectional boundary.

To enable fully automated livestock body measurement, this study proposes a spatial localization-based strategy formulated within a ground-referenced coordinate system. The input to the framework is the point-cloud segmentation output generated by Omni-PointMamba. Specifically, Omni-PointMamba is first employed to decompose the raw point cloud into livestock body points and ground points, thereby removing background clutter. As illustrated in Figure 5, an anatomical coordinate system is subsequently established using the ground plane as a geometric reference. The z-axis is aligned with the estimated ground normal vector to ensure vertical consistency across samples. The lateral axis (y-axis) is then defined by projecting the farthest point pair on the livestock torso onto the horizontal plane and taking the orthogonal direction as the lateral orientation. Finally, the longitudinal axis (x-axis) is determined using the head point cloud as a directional prior, aligning the coordinate system with the anatomical head-to-tail direction.

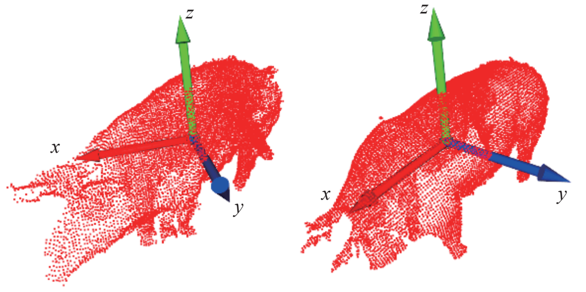

a. Coordinate system of the point cloud of the initial pig b. Coordinate system after correction

Figure 5 Schematic diagram of coordinate correction based on the segmentation result

After coordinate normalization, a clustering-driven spatial localization strategy is employed to achieve a coarse-to-fine partition of measurement-relevant regions. For each individual, k-means clustering with two centroids is first applied to the body point cloud, separating it into anterior (head-oriented) and posterior (tail-oriented) halves. A second-stage k-means clustering is then performed independently within each trunk region with three centroids, further refining local anatomical structures and improving spatial separability. As illustrated in Figure 3 and Figure 6, this hierarchical clustering procedure subdivides the livestock body into six subregions. Following the two-stage partitioning, clusters corresponding to the forelimbs and hind limbs are excluded through a geometric filtering procedure. Guided by the normalized anatomical coordinate system, the remaining anterior trunk region is used for shoulder width estimation, whereas the posterior trunk region is used for hip width estimation. This hierarchical clustering-based localization mechanism enables stable anatomical region identification without reliance on manually annotated landmarks, thereby ensuring consistent support for subsequent keypoint extraction and geometric measurement.

a. Clustering results of the first step b. Clustering results of the second step

Figure 6 Schematic diagram of different clustering centers

2.3.1 Body measurement of Landrace pigs

As shown in Figure 3, the main measurement indicators of pigs include body width, hip width, and chest circumference. Specifically, the spatial positioning measurement method obtains the straight-line body width and hip width of pigs by determining the Euclidean distance in the y-axis direction between the key points α_0 and α_1 in the point cloud facing the head and the key points b_0 and b_1 in the point cloud facing the tail.

The chest circumference of pigs is measured by the arc circumference at the junction of the front legs and the abdomen of pigs, as shown in Figure 7. A plane in the y-axis direction is constructed, which is horizontal to the plane formed by the two points c_0 and c_1. The intersection curve between the constructed plane and the point cloud of the pig is used to calculate the chest circumference. Its calculation formula is:

$$C_{\text{chest}} = 2\pi r_2 + 4(r_1 + r_2) \tag{12}$$

where, r_1 is the major axis radius of the fitted ellipse, r_2 is the minor axis radius of the fitted ellipse, and C_{chest} is the chest circumference of the pig.

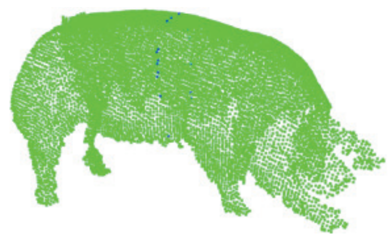

Figure 7 Diagram of chest circumference measurement

2.3.2 Body measurement of Hereford cattle

For cattle, different from the body measurement parameters of pigs, the oblique body length, chest width, hip length, and heart girth are taken into account, as shown in Figure 4. The oblique body length of cattle is defined as the straight-line Euclidean distance between the point d_0' and the point d_1'. The chest width of cattle is obtained by the Euclidean distance in the y-axis direction between a_0' and a_1'. The hip length of cattle is obtained by the Euclidean distance from the tail root point d_1' to the ground. The heart girth of cattle is measured in the same way as the chest circumference of pigs, which is composed of the connection points at the junction of the legs and the abdomen where the front legs meet the abdomen.

2.4 Evaluation setting

All comparative experiments are conducted on a workstation with NVIDIA GeForce RTX 4090 and Intel Core i7-12700. The deep learning framework PyTorch is used to train the network in a server environment. The network is optimized using the Adam optimizer. The initial learning rates are set to 0.0001. In the point cloud segmentation stage, the number of Conv blocks and Point Mamba blocks in the proposed Omni-PointMamba is set to $L=4$.

Four groups of experiments have been designed: a. This study divides the point cloud dataset of 200 pigs into three subsets, including a training set consisting of 150 samples, a validation set consisting of 30 samples, and a test set consisting of 20 samples; b. The 103 point cloud of cattle are divided into a training set with 70 samples, a validation set with 23 samples, and a test set with 20 samples; c. The training set of 150 Landrace pig samples and the test set of 20 cattle samples are combined into a new training set. The validation set of 30 samples and the validation set of 23 cattle samples are combined into a new validation set, and the training set of 70 cattle samples is used as the test set of the experiment; d. The training set of 70 cattle samples and the test set of 20 pig samples are combined into a new training set. The validation set of 30 Landrace pig samples and the validation set of 23 cattle samples are combined into a new validation set, and the training set of 150 Landrace pig samples is used as the test set.

In this study, the spatial localization measurement method is compared with the traditional manual measurement method for body size measurement. It enables automatic extraction of individual body size parameters by leveraging the segmentation outputs from Omni-PointMamba. By combining these segmentation results with the ground normal vector, the coordinate system of each animal is normalized, and key body measurement points are identified using the k-means clustering algorithm.

2.5 Evaluation metrics

The validation performance of point cloud segmentation is quantified using the mean intersection over union (mIoU) metric. Its formula is expressed as follows:

$$mIoU = \frac{1}{C}\sum_{c=1}^{C}\frac{|\{y=C\}\cap\{t=C\}|}{|\{y=C\}\cup\{t=C\}|} \tag{13}$$

where, $\{y=C\}$ is the set belonging to class C in the predicted region; $\{t=C\}$ denotes the set of points in class C according to the truth label; C is the number of segmentation categories.

In addition, the experiment also uses the mean absolute percentage error (MAPE), the root mean square error (RMSE), and the coefficient of determination (R^2) to evaluate the predictive performance by comparing predicted and actual values. These metrics are formulated as:

$$\text{MAPE} = \frac{1}{y}\sum_{i=1}^{n}\left|\frac{y_i-\hat{y}_i}{y_i}\right| \tag{14}$$

$$\text{RMSE} = \sqrt{\frac{1}{n}\sum_{i=1}^{n}(y_i-\hat{y}_i)^2} \tag{15}$$

$$R^2 = 1-\frac{\sum_{i=1}^{n}(y_i-\hat{y}_i)^2}{\sum_{i=1}^{n}(y_i-\bar{y}_i)^2} \tag{16}$$

where, y_i is the actual observed value, $\hat{y}_i$ is the predicted value, $\bar{y}$ is the mean value of the observed values, and n is the number of samples. The value range of R^2 ranges from 0 to 1, and higher values indicate better goodness of fit.

3 Results

3.1 Livestock body point-cloud segmentation results

The performance of the proposed Omni-PointMamba is evaluated through quantitative and qualitative comparisons using point cloud data from the Landrace pig dataset and Hereford cattle dataset. A series of models are selected for comparison such as PointNet[15], PointNet++[28], PointCNN[16], PointMLP[29], Point Transformer[30], and PointMamba[23].

The segmentation performance on the pig dataset is reported in Table 1. Omni-PointMamba achieves an overall mIoU of 0.9930, with ground and pig segmentation mIoUs of 0.9920 and 0.9940, respectively, outperforming all competing methods. Traditional architectures such as PointNet and PointNet++ exhibit relatively inferior performance, which may be attributed to their point-wise feature extraction mechanisms that limit global structural modeling capability. Notably, within the proposed measurement-oriented framework, the objective of segmentation extends beyond maximizing global mIoU. Instead, it focuses on ensuring robust body–ground separation and preserving structurally complete livestock contours to support subsequent geometric measurement.

Table 1 The segmentation result on the Landrace pig dataset

Methods	Ground mIoU	Pig mIoU	mIoU
K-means[31]	0.9031	0.9002	0.8911
PointNet[15]	0.9826	0.9869	0.9848
PointNet++[28]	0.9865	0.9906	0.9886
PointCNN[16]	0.9610	0.9720	0.9665
PointMLP[29]	0.9825	0.9885	0.9855
Point Transformer[30]	0.9896	0.9933	0.9915
PointMamba[23]	0.9905	0.9935	0.9920
Omni-PointMamba	**0.9920**	**0.9940**	**0.9930**

Table 2 presents the segmentation performance on the Hereford cattle dataset. Compared with the pig dataset, this scenario involves more complex structural variations and denser point distributions. Under these challenging conditions, Omni-PointMamba achieves an overall mIoU of 0.9685, with ground and cattle mIoU values of 0.9613 and 0.9757, respectively, demonstrating clearer improvements over competing baselines. The larger performance margin observed on the cattle dataset suggests that the proposed omnidirectional scanning mechanism improves robustness in the presence of increased geometric complexity. These findings further indicate that stable segmentation and well-preserved boundary structures are critical for ensuring consistent performance in subsequent measurement tasks.

Table 2 The segmentation result on the Hereford cattle dataset

Methods	Ground mIoU	Cattle mIoU	mIoU
K-means[31]	0.8140	0.8044	0.8612
PointNet[15]	0.8548	0.8676	0.8612
PointNet++[28]	0.9075	0.9093	0.9034
PointCNN[16]	0.9103	0.9195	0.9169
PointMLP[29]	0.9227	0.9423	0.9325
Point Transformer[30]	0.9180	0.9455	0.9317
PointMamba[23]	0.9334	0.9293	0.9264
Omni-PointMamba	**0.9613**	**0.9757**	**0.9685**

Figure 8 illustrates the visual segmentation results of a Landrace pig point cloud sample. In this figure, red denotes ground points, black denotes points belonging to the livestock body, and green represents misclassified points. To improve the interpretability of the visualization results, the RGB image and the corresponding ground truth are further included for comparison. It can be observed that all methods are generally able to achieve a basic separation between the livestock body and the ground. However, the misclassified points are mainly concentrated in the lower abdominal region, around the limbs, and in boundary areas where the animal body is close to the ground, indicating that these regions remain the major challenges affecting segmentation accuracy. Compared with the competing methods, Omni-PointMamba produces the fewest misclassified points, with errors distributed in a more localized manner, demonstrating superior stability in preserving the body contour of the livestock and suppressing interference from the ground background.

Figure 9 presents the visual segmentation results of a cattle point cloud sample. Overall, all methods are able to recover the main body contour of the cattle to a certain extent. However, segmentation errors remain in structurally complex regions, such as the lower abdominal boundary, the distal parts of the limbs, and the near-ground boundary areas, indicating that these regions continue to be the key challenges limiting further improvement in segmentation accuracy. Compared with the competing methods, Omni-PointMamba produces results that are closer to the ground truth and demonstrates superior stability in preserving the body contour, recovering local structural details, and suppressing ground-background interference. These results indicate that the proposed method can more effectively model the local geometric characteristics and global structural relationships in cattle point clouds, thereby providing a more reliable segmentation basis for subsequent body measurement tasks.

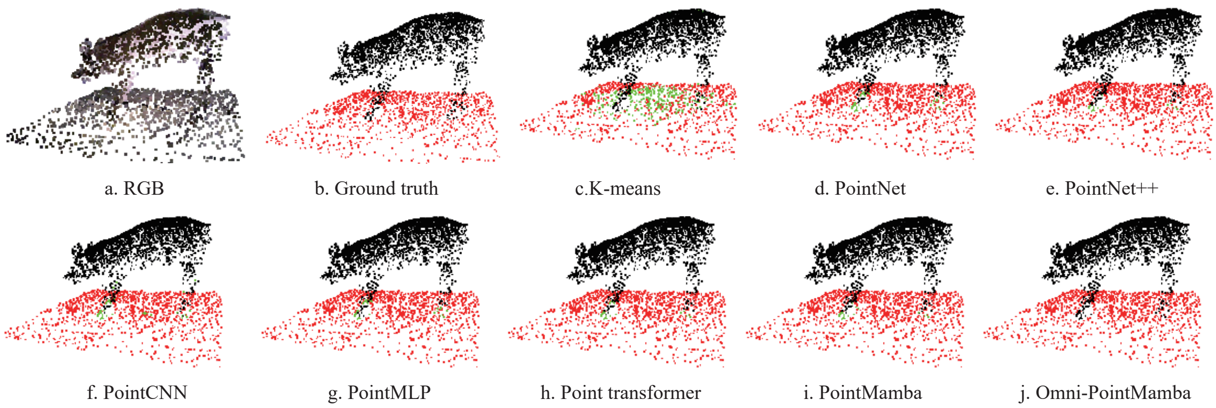

Figure 8 The segmentation map of the Landrance pig point cloud dataset

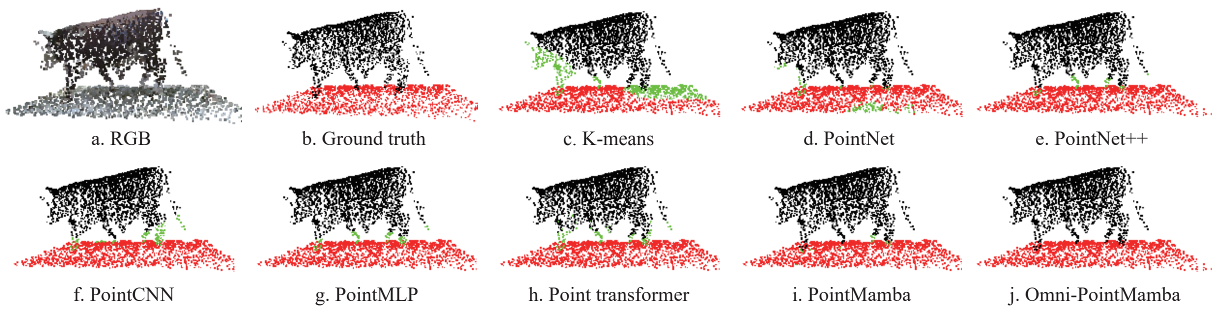

Figure 9 The segmentation map of the Herford cattle point cloud dataset

To further substantiate the effectiveness of the proposed two-stage segmentation framework, a single-stage baseline is implemented for direct comparison. In the single-stage setting, all points are directly classified into fine-grained semantic categories, including head, left ear, right ear, torso, forelegs, hind legs, tail, ground, and background. For fair comparison, both the single-stage and two-stage variants share identical backbone architectures, training protocols, and evaluation metrics.

As reported in Table 3, single-stage segmentation can achieve strong overall mIoU, especially on the Landrace pig dataset. However, the two-stage design is introduced primarily to better handle anatomically small or shape-sensitive regions (e.g., head and tail) by decoupling coarse foreground extraction from fine-grained part parsing. This hierarchical formulation helps reduce category interference between livestock parts and background-related classes, and is beneficial for refining structural boundaries that are critical to subsequent measurement.

3.2 Cross-domain evaluation

In this study, comparative experiments were performed on the point cloud datasets of Hereford cattle and Landrace pigs, with the results presented in Figures 10 and 11. The Omni-PointMamba model demonstrates markedly superior performance to mainstream point cloud models (including the PointNet series, PointCNN, PointTransformer, etc.) in segmenting key parts of the two livestock types, such as the toe-ground intersection and livestock abdomen. Regarding the Hereford cattle data, Omni-PointMamba (Figure 11h) preserves the integrity of the trunk body contour. In contrast, PointNet exhibits more ambiguous points, predominantly at the junction of the abdomen, leg, and ground. As for the pig data, Omni-PointMamba achieves noise-free segmentation at the leg-ground junction and the body-background boundary. However, the comparison models (PointNet, PointNet++, PointCNN, PointMLP, PointTransformer) display discrete mis-segmentation points. It should be noted that although Omni-PointMamba delivers better overall segmentation, it still exhibits localized confusion in the foreleg-ground junction region.

Table 4 shows the cross-domain experimental results of the cattle dataset. It shows that Omni-PointMamba achieves a mIoU of 0.9733, with a ground mIoU of 0.9714 and a pig mIoU of 0.9760, outperforming all other models. In addition, the performance of PointMamba is also very competitive, validating the effectiveness of the Mamba-based segmentation backbone. The PointMamba outperforms MLP-based models, including PointNet, PointNet++, and pointMLP, as well as point convolution-based models such as PointCNN, and Transformer-based models. These results further highlight the advantages of omni-selective scanning methods and Mamba-based designs in improving cross-species segmentation accuracy, especially in complex livestock datasets.

Then, the model is trained on the cattle dataset and tested on the pig dataset. The evaluation metrics of the segmentation results are shown in Table 5. Among the evaluated models, Omni-PointMamba achieves the highest performance in all metrics, with an mIoU of 0.9033, a ground class mIoU of 0.8976, and a pig class mIoU of 0.9090, showing the strong ability of the model to transform feature domains from pigs to cattle. At the same time, PointMamba also shows competitive results, verifying the effectiveness of point cloud segmentation based on the Mamba structure. Although PointNet can produce segmentation results that are usable for basic geometric measurement after simple post-processing, the practical objective of the proposed framework is to enhance measurement robustness rather than merely achieve feasible segmentation. In measurement-oriented tasks, small segmentation inconsistencies at structurally sensitive regions—such as the abdomen-leg-ground junction and limb boundaries—may influence clustering-based trunk localization and subsequently affect shoulder and hip key-point stability. As illustrated in Figures 9 and 10, Omni-PointMamba provides more continuous contour delineation and cleaner separation at these critical interfaces compared with PointNet and other baselines. This structural consistency reduces error propagation during the subsequent two-stage localization process, thereby improving measurement reliability, especially in cross-domain scenarios where morphological variations and pose differences are more pronounced.

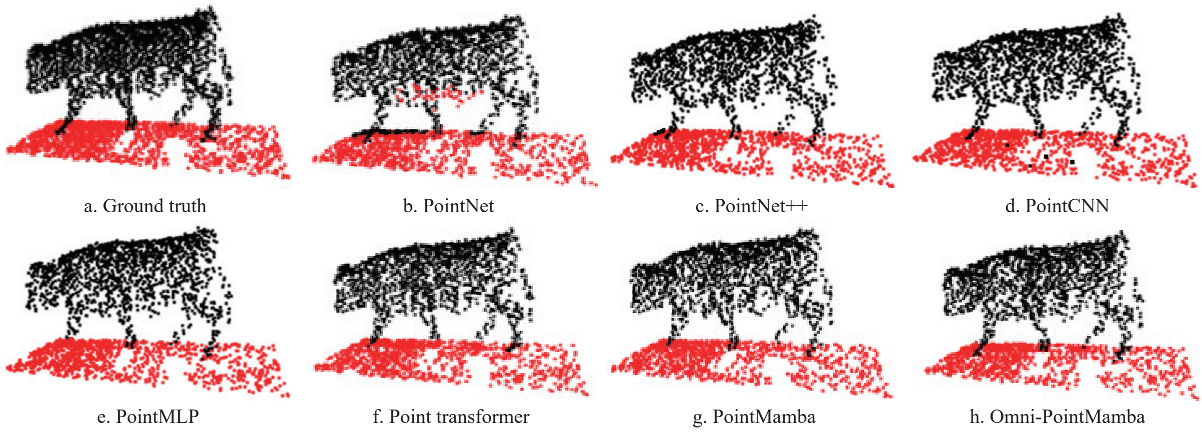

Figure 10 The cross-domain segmentation map of the Herford cattle point cloud dataset

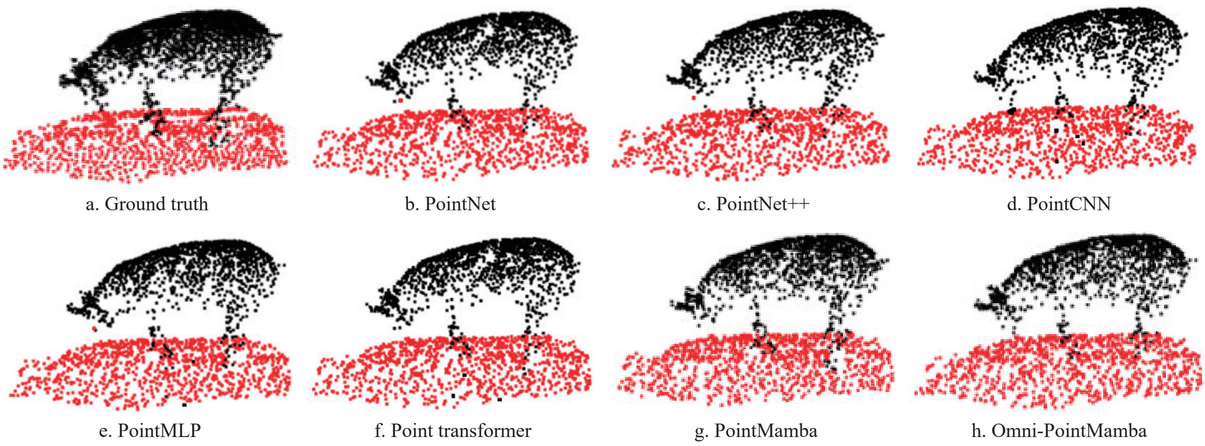

Figure 11 The cross-domain segmentation map of the Landrace pig point cloud dataset

Table 3 The segmentation result on the Hereford cattle dataset

Methods	One-stage		Two-stage	
	mIoU for Landrace pig	mIoU for Hereford cattle	mIoU for Landrace pig	mIoU for Hereford cattle
PointNet[15]	0.9848	0.8612	0.8545	0.8108
PointNet++[28]	0.9886	0.9034	0.8837	0.9073
PointCNN[16]	0.9665	0.9169	0.9433	0.9211
PointMLP[29]	0.9855	0.9325	0.9518	0.9186
Point Transformer[30]	0.9915	0.9317	0.9367	0.8980
PointMamba[23]	0.9920	0.9264	0.9431	0.9118
Omni-PointMamba	0.9930	0.9685	0.9611	0.9465

Therefore, the advantage of Omni-PointMamba lies not only in marginal metric improvements, but in delivering structurally stable segmentation that better supports automated and consistent body measurement across heterogeneous livestock datasets.

Table 4 The cross-domain segmentation result on the Hereford cattle point cloud dataset

Methods	Ground mIoU	Cattle mIoU	mIoU
PointNet	0.9220	0.9203	0.9237
PointNet++	0.9313	0.9194	0.9232
PointCNN	0.9162	0.8968	0.9356
PointMLP	0.9539	0.9526	0.9552
Point Transformer	0.9617	0.9599	0.9635
PointMamba	0.9635	0.9600	0.9670
Omni-PointMamba	**0.9733**	**0.9714**	**0.9760**

3.3 Livestock body measurement results

Body estimation is conducted using point cloud data of Landrace pigs and Hereford cattle in standard upright postures. Manual measurements are used as reference standards to evaluate the performance of the spatial localization-based measurement method. Based on the segmented point clouds, we select 10 pigs and calculate the MAPE for three body measurement parameters: body width (REbw), hip width (REhw), and chest circumference (REcc). Similarly, 10 cattle are randomly selected to evaluate the MAPE for oblique body length (REobl), chest width (REcw), hip height (REhh), and heart girth (REhg).

Table 5 The cross-domain segmentation result on the Landrace pig point cloud dataset

Methods	Ground mIoU	Cattle mIoU	mIoU
PointNet	0.8273	0.8318	0.8296
PointNet++	0.8258	0.8308	0.8283
PointCNN	0.8032	0.8638	0.8332
PointMLP	0.8275	0.8325	0.8300
Point Transformer	0.8690	0.8729	0.8709
PointMamba	0.8781	0.8857	0.8819
Omni-PointMamba	**0.8976**	**0.9090**	**0.9033**

As shown in Table 6, the body measurement results for pigs demonstrate that the proposed model achieves REbw of 1.34%, 1.99% for REhw, and 1.37% for REcc. These results indicate that the spatial localization-based measurement method performs well across key body size parameters, with particularly high accuracy in body width estimation. The REhw value of 1.99% suggests that hip boundary recognition may be affected by the quality of the point cloud or variations in animal posture. At the individual level, most measurement errors fall within an acceptable range, with samples 1, 2, and 3 all showing errors below 2%. However, higher hip width errors are observed in samples 4 and 8, at 3.32% and 3.47% respectively, primarily due to missing point cloud data. Chest circumference estimates remain relatively stable, reflecting the model's robustness in capturing body girth features. Overall, the coefficient of R^2 for all measurements exceeds 0.95, confirming the reliability and accuracy of the proposed measurement approach.

As listed in Table 7, the MAPE for the four body measurement parameters of cattle REobl, REcw, REhh, and REhg are 2.24%, 3.28%, 2.18%, and 4.22%, respectively. The results for REobl and REhh remain consistently within the range of 2% to 4%, demonstrating that the spatial localization-based measurement method can effectively handle posture variation and environmental noise. Additionally, REcw and REhg fall within the acceptable range for practical implementation in livestock farming, indicating the method's adaptability in capturing key circumference traits. At the individual level, most samples exhibit low measurement errors, with particularly stable results observed in oblique length and hip height. These findings confirm the robustness of the proposed method across different individuals.

Table 6 The body measurement results for the Landrace pig dataset

ID	Manual measurement/cm			Spatial positioning measurement/cm			Individual measurement results/%		
	Body width	Hip width	Chest circumference	Body width	Hip width	Chest circumference	REbw	REhw	REcc
1	29.18	25.27	120.0	28.86	26.39	114.39	1.10	2.06	2.18
2	30.81	30.80	115.0	30.76	30.26	111.16	0.16	1.75	3.34
3	27.28	32.81	105.0	26.88	32.83	104.15	1.47	0.06	0.81
4	30.64	26.51	115.0	30.77	27.39	111.45	0.42	3.32	1.35
5	29.19	29.15	106.0	29.11	28.61	105.63	0.27	1.85	0.35
6	27.10	24.05	101.0	26.65	23.71	102.02	1.66	1.41	1.01
7	23.48	25.96	102.0	24.12	26.39	103.77	2.73	1.66	1.74
8	28.52	30.23	103.0	29.96	31.28	102.31	3.65	3.47	0.67
9	29.73	27.65	103.4	30.24	28.04	106.36	1.72	1.41	2.09
10	28.94	25.53	111.0	30.01	27.97	110.86	0.24	2.90	0.13
MAPE	-	-	-	-	-	-	1.34	1.99	1.37
RMSE	-	-	-	-	-	-	0.57	0.65	2.70
R^2	-	-	-	-	-	-	0.95	0.96	0.95

Table 7 The body measurement results for the Hereford cattle dataset

ID	Manual measurement/cm				Spatial positioning measurement/cm				Individual measurement results/%			
	Body oblique length	Chest width	Hip height	Heart girth	Body oblique length	Chest width	Hip height	Heart girth	REobl	REcw	REhh	REhg
1	145.00	40.00	122.00	172.00	141.50	40.20	125.70	167.20	2.38	0.38	3.06	2.78
2	127.00	39.00	121.00	171.00	123.80	37.30	124.10	168.10	2.51	4.45	2.61	1.696
3	128.00	43.00	121.00	176.00	123.20	46.10	118.70	179.70	3.72	7.13	1.93	2.07
4	150.00	46.00	123.00	176.00	146.20	47.90	125.20	175.20	2.50	4.15	1.90	8.96
5	140.00	41.00	127.00	178.00	142.90	39.50	124.70	170.30	2.06	3.71	1.82	4.31
6	138.00	43.00	124.00	178.00	134.30	42.20	128.70	166.40	2.71	1.78	3.79	6.54
7	149.00	41.00	121.00	172.00	149.00	40.50	119.30	164.90	0.01	1.27	1.39	4.15
8	137.00	48.00	117.00	172.00	140.50	45.60	116.90	170.70	2.55	4.90	0.08	0.74
9	140.00	44.00	120.00	175.00	143.50	42.40	124.60	164.10	2.55	3.62	3.86	6.21
10	151.00	46.00	122.00	182.00	148.80	45.30	125.90	190.70	1.43	1.41	3.18	4.78
MAPE	-	-	-	-	-	-	-	-	2.24	3.28	2.18	4.22
RMSE	-	-	-	-	-	-	-	-	3.33	1.67	3.16	8.57
R^2	-	-	-	-	-	-	-	-	0.94	0.86	0.64	0.58

4 Discussion

Earlier studies have explored body size estimation in various livestock species including chickens, pigs, sheep, and cattle based on RGB imagery. However, RGB images are inherently limited in representing high-dimensional spatial information, which restricts their ability to capture detailed body morphology. As a result, research in this area has gradually shifted toward the use of 3D point cloud data.

Wang et al. proposed an automatic method to measure pig chest circumference using point cloud segmentation and posture normalization, achieving an average relative error of 7.87%[32]. Weng et al. developed a cattle body measurement system based on a dynamic unbalanced octree grouping segmentation model, enabling the estimation of body length, shoulder height, and hip height with relative errors below 2.6%[33]. Han et al. proposed Shapewarp, a global-to-local non-rigid posture correction framework for sheep point clouds. On 30 sheep, R^2 values for five body measurement parameters improved by 11.47%, 11.28%, 10.94%, 32.09%, and 10.83%, respectively[34]. Hou et al. proposed CattlePartNet, a PointNet-based network for segmenting cattle body parts[35]. Combined with contour extraction, it estimated body measurements with MAPEs of 4.96%, 5.47%, and 6.04% for height, length, and chest circumference. Lu et al. introduced a two-stage GCN-based method for cattle body measurement, achieving 3.58% MAPE on nine parameters across 100 cattle[36].

Beyond the above comparisons, the value of the proposed method lies in its measurement-oriented integration of segmentation and geometric computation within a unified pipeline. Unlike approaches that treat segmentation as an isolated module, the proposed framework explicitly links segmentation quality to downstream anatomical localization and keypoint determination. This design mitigates error propagation from boundary ambiguity to measurement estimation. The omnidirectional scanning mechanism enhances structural continuity and contour completeness in geometrically sensitive regions. As a result, it provides more stable geometric inputs for automated body measurement, particularly under cross-species morphological and postural variations.

It should be noted that the practical applicability of the proposed method does not strictly depend on the clear visibility of all measurement keypoints in a local sense. Instead, the method mainly benefits from the overall geometric boundary of the livestock body, contour continuity, and the separation between the body and the ground background after segmentation. Therefore, even when local appearance cues around some keypoints are weakened or partially invisible due to posture variation, the proposed framework can still provide a useful basis for body measurement as long as the overall body contour and measurement-relevant regions remain sufficiently preserved. Nevertheless, when severe self-occlusion, extreme poses, or substantial local point missingness occur, the reliability of boundary-based anatomical localization and subsequent measurement may decrease. In this sense, the current method is more suitable for non-contact measurement scenarios in which the livestock body contour is relatively complete and the body–ground boundary can be stably recovered.

Despite these advantages, several limitations remain. The current implementation still relies on clustering-based region localization and may be affected when severe occlusion, extreme pose variation, or substantial local boundary degradation is present. In such cases, the stability of anatomical localization and body measurement may decrease. In addition, broader validation across more species and farm environments, as well as further efficiency optimization for large-scale deployment, will be explored in future work.

5 Conclusions

To improve the automation and precision of livestock body measurement, this study presents a two-stage framework that combines the Omni-PointMamba point cloud segmentation model with a spatial localization measurement method, enabling efficient non-contact body measurement in complex farming environments. The Omni-PointMamba model integrates an omnidirectional scanning strategy with a dual-feature extraction structure that captures both global shape and local geometric details, thereby supporting accurate separation of livestock from the background. On the public available pigs and cattle datasets, the model achieves mIoU scores of 0.9930 (pigs) and 0.9685 (cattle), outperforming six widely used deep learning models, and providing a robust foundation for subsequent parameter estimation. The spatial localization measurement method constructs a measurement coordinate system using the ground normal vector and employs a two-step clustering strategy to automatically identify key anatomical regions. Without manual intervention, the framework estimates parameters like body width and hip width, achieving MAPEs of 1.99% and 4.22%. The results indicate strong adaptability to variations in livestock morphology and confirm the effectiveness and practicality of the method in cross-species applications, paving the way for the development of intelligent precision farming technologies.

This study focuses on animals in upright postures. Under extreme non-ideal conditions such as twisting or lying down, point cloud sparsity may reduce the accuracy of keypoint detection. Further research will integrate pose estimation techniques to improve the adaptability of the system under suboptimal pose scenarios, thereby increasing the scalability of automated measurement frameworks in agricultural operations.

Acknowledgements

This work was supported by the Ministry of Science and Technology of China as part of the Science and Technology Innovation 2030–Major Project of “New Generation Artificial Intelligence” (No. 2021ZD0113701).

[References]

[1] Chu M Y, Si Y S, Li Q, Liu G. Research advances in the automatic measurement technology for livestock body size. Transactions of the Chinese Society of Agricultural Engineering, 2022; 38(13): 228–240. (in Chinese)
[2] Liu D, He D J, Norton T. Automatic estimation of dairy cattle body condition score from depth image using ensemble model. Biosystems Engineering, 2020; 194: 16–27.
[3] Salau J, Haas J H, Junge W, Thaller G. Extrinsic calibration of a multi-Kinect camera scanning passage for measuring functional traits in dairy cows. Biosystems Engineering, 2016; 151: 409–424. doi: 10.1016/j.biosystemseng. 2016;10.008.
[4] Nir O, Parmet Y, Werner D, Adin G, Halachmi I. 3D computer-vision system for automatically estimating heifer height and body mass. Biosystems Engineering, 2018; 173: 4–10.
[5] Wang T H, Chen B, Zhang Z Q, Li H, Zhang M. Applications of machine vision in agricultural robot navigation: A review. Computers and Electronics in Agriculture, 2022; 198: 107085.
[6] Zhan L N, Wu P, Wuyun T, Jiang X H, Xuan C Z, Ma Y H. Algorithm of sheep body dimension measurement and its applications based on image analysis. Computers and Electronics in Agriculture, 2018; 153: 33–45.
[7] Xie C Q, Cang Y J, Lou X Z, Xiao H, Xu X, Li X J, et al. A novel approach based on a modified mask R-CNN for the weight prediction of live pigs. Artificial Intelligence in Agriculture, 2024; 12: 19–28. doi: 10.1016/j.aiia.20 24.03.001
[8] Li R, Wen Y C, Zhang S J, Xu X S, Ma B L, Song H B. Automated measurement of beef cattle body size via key point detection and monocular depth estimation. Expert Systems with Applications, 2024; 244: 123042.

[9] Salau J, Haas J H, Junge W, Thaller G. A multi-Kinect cow scanning system: Calculating linear traits from manually marked recordings of Holstein-Friesian dairy cows. Biosystems Engineering, 2017; 157: 92–98.

[10] le Cozler Y, Allain C, Caillot A, Delouard J M, Delattre L, Luginbuhl T, et al. High-precision scanning system for complete 3D cow body shape imaging and analysis of morphological traits. Computers and Electronics in Agriculture, 2019; 157: 447–453.

[11] Yang G Y, Xu X S, Song L, Zhang Q R, Duan Y C, Song H B. Automated measurement of dairy cows body size via 3D point cloud data analysis. Computers and Electronics in Agriculture, 2022; 200: 107218.

[12] Wang Y X, Shi Y Y, Chen Z D, Wu Z F, Cai G Y, Zhang S M, et al. Pig back transformer: Automatic 3D pig body measurement model. Smart Agriculture, 2024; 6(4): 76–90.

[13] Du A, Guo H, Lu J, Su Y, Ma Q, Ruchay A, et al. Automatic livestock body measurement based on keypoint detection with multiple depth cameras. Computers and Electronics in Agriculture, 2022; 198: 107059.

[14] Li J W, Ma W H, Bai Q, Tulpan D, Gong M L, Sun Y, et al. A posture-based measurement adjustment method for improving the accuracy of beef cattle body size measurement based on point cloud data. Biosystems Engineering, 2023; 230: 171–190.

[15] Qi C R, Su H, Mo K, Guibas L J. PointNet: Deep learning on point sets for 3D classification and segmentation. In: 2017 IEEE Conference on Computer Vision and Pattern Recognition (CVPR), Honolulu, HI, USA: IEEE, 2017; pp.77–85. doi: 10.1109/CVPR.2017.16.

[16] Li Y Y, Bu R, Sun M C, Wu W, Di X H, Chen B Q. PointCNN: Convolution on X-transformed points. In: Proceedings of the 32nd International Conference on Neural Information Processing Systems (NIPS' 18). Red Hook, NY, USA: Curran Associates Inc., 2018; pp.828–838.

[17] Wu W X, Qi Z G, Li F X. PointCONV: Deep convolutional networks on 3D point clouds. In: 2019 IEEE/CVF Conference on Computer Vision and Pattern Recognition (CVPR), Long Beach, CA, USA: IEEE, 2019; pp.9613–9622. doi: 10.1109/CVPR.2019.00985.

[18] Lin Z H, Huang S Y, Wang Y C F. Learning of 3D graph convolution networks for point cloud analysis. IEEE Transactions on Pattern Analysis and Machine Intelligence, 2022; 44: 4212–4224.

[19] Xu Q G, Sun X D, Wu C Y, Wang P Q, Neumann U. Grid-GCN for fast and scalable point cloud learning. In: 2020 IEEE/CVF Conference on Computer Vision and Pattern Recognition (CVPR), Seattle, WA, USA: IEEE, 2020; pp.5660–5669. doi: 10.1109/CVPR42600.2020.00570.

[20] Wu P X, Chai B S, Li H B, Zheng M H, Peng Y S, Wang Z Y, et al. Spiking point transformer for point cloud classification. Proceedings of the AAAI Conference on Artificial Intelligence, 2025; 39(20): 21563–21571.

[21] Zhao H S, Li J, Jia J Y, Torr P, Koltun V. Point transformer. In: 2021 IEEE/CVF International Conference on Computer Vision (ICCV), Montreal, QC, Canada: IEEE, 2021; pp.16239–16248, doi: 10.1109/ICCV48922.2021.01595.

[22] Zeng Z X, Wu Z M, Xie R T, Lin K, Tan S W, He X Y, et al. MACA-Net: Mamba-driven adaptive cross-layer attention network for multi-behavior recognition in group-housed pigs. Agriculture (Switzerland), 2025; 15(9): 968. doi: 10.3390/agriculture15090968.

[23] Bai X, Liang D K, Tan X, Xu W, Ye X Q, Zhou X, et al. PointMamba: A simple state space model for point cloud analysis. In: Advances in Neural Information Processing Systems 37, Vancouver, Canada: Neural Information Processing Systems Foundation, Inc. (NeurIPS), 2024; 32653–32677. doi: 10.52202/079017-1026

[24] Zhang T, Yuan H B, Qi L, Zhang J N, Zhou Q Y, Ji S P, et al. Point cloud mamba: Point cloud learning via state space model. Proceedings of the AAAI Conference on Artificial Intelligence, 39(10): 10121–10130. doi: 10.1609/aaai.v39i10.33098

[25] Wang K, Guo H, Ma Q, Su W, Chen L C, Zhu D H. A portable and automatic Xtion-based measurement system for pig body size. Computers and Electronics in Agriculture, 2018; 148: 291–298.

[26] Ruchay A, Kober V, Dorofeev K, Kolpakov V, Miroshnikov S. Accurate body measurement of live cattle using three depth cameras and non-rigid 3-D shape recovery. Computers and Electronics in Agriculture, 2020; 179: 105821.

[27] Lyons T, Cirone N M, Orvieto A, Salvi C, Walker B. Theoretical foundations of deep selective state-space models. In: Advances in Neural Information Processing Systems 37, Vancouver, Canada: Neural Information Processing Systems Foundation, Inc. (NeurIPS), 2024; pp.127226–127272.

[28] Qi C R, Yi L, Su H, Guibas L J. PointNet++: Deep hierarchical feature learning on point sets in a metric space supplementary material. arXiv: 1706.02413, 2017: In Press. doi: 10.48550/arXiv.1706.02413.

[29] Ma X, Qin C, You H X, Ran H X, Fu Y. Rethinking network design and local geometry in point cloud: A simple residual MLP framework. arXiv: 2202.07123, 2022; In press. doi: 10.48550/arXiv.2202.07123.

[30] Engel N, Belagiannis V, Dietmayer K. Point transformer. IEEE Access, 2021; 9: 134826–134840.

[31] Liu Y, Zhou J, Bian Y F, Wang T S, Xue H X, Liu L S. Estimation of weight and body measurement model for pigs based on back point cloud data. Animals, 2024; 14: 1046.

[32] Wang K, Zhu D H, Guo H, Ma Q, Su W, Su Y. Automated calculation of heart girth measurement in pigs using body surface point clouds. Computers and Electronics in Agriculture, 2019; 156: 565–573.

[33] Weng Z, Lin W Z, Zheng Z Q. Cattle body size measurement based on DUOS–PointNet++. Animals, 2024; 14(17): 2553.

[34] Han B B, Zhang J R, Xiang Y Y, Li X P, Li S Q. Shapewarp: A "global-to-local" non-rigid sheep point cloud posture rectification method. Expert Systems with Applications, 2025; 270: 126524.

[35] Hou Z X, Zhang Q, Zhang B, Zhang H M, Huang L W, Wang M L. CattlePartNet: An identification approach for key region of body size and its application on body measurement of beef cattle. Computers and Electronics in Agriculture, 2025; 232: 110013.

[36] Lu H X, Zhang J L, Yuan X F, Lv J H, Zeng Z W, Guo H, et al. Automatic coarse-to-fine method for cattle body measurement based on improved GCN and 3D parametric model. Computers and Electronics in Agriculture, 2025; 231: 110017.